Sādhanā (2020)45:175
https://doi.org/10.1007/s12046-020-01415-0

Photo sensitizing and electrochemical performance analysis of mixed natural dye and nanostructured ZnO based DSSC

DOLA SINHA[1,*], DEBASIS DE[2,4] and ABDUL AYAZ[3]

[1]Department of Electrical Engineering, Dr. B. C. Roy Engineering College, Durgapur, India
[2]Department of Applied Electronics and Instrumentation Engineering, Dr. B. C. Roy Engineering College, Durgapur, India
[3]Department of Electrical Engineering, Rampurhut Govt. Polytechnic College, Birbhum, India
[4]Energy Institute Bangalore, A centre of Rajiv Gandhi Institute of Petroleum Technology, VTU PG Campus, Chikkabalapura, India
e-mail: dola.sinha@bcrec.ac.in; debasis.ju@gmail.com; aayaz1962@gmail.com

MS received 29 October 2018; revised 7 March 2020; accepted 15 May 2020

Abstract. The paper highlights the enactment of the natural dyes, like purple cabbage, spinach, turmeric and their mixture as a photo-sensitizer, with nanostructured zinc oxide (ZnO) as a photo-anode, based dye-sensitized solar cell (DSSC). The field emission scanning electron microscopic image of ZnO, prepared by chemical bath deposition process, proclaims two different types of morphology, nano-wire and nano-plate shape. The photo sensitizing properties of the natural dyes and their mixed part are explored through FTIR spectra and UV-vis light absorbance characteristics. The FTIR spectra explore the presence of different anchoring chemical groups which confirm the strong anchoring bond with ZnO and enhancement of electron mobility. The diffused reflectance spectra (DRS) of dye-loaded ZnO films incisive the absorption of dye on the mesoporous ZnO surface. The relative energy band positions of individual and mixed dye, yield stable execution of the cell that has been performed through the cyclic voltammeter. The driving force energy requirement for effortless transport of electron from the mixed dye to the conduction band of ZnO is revealed lowers (0.34 eV) as compared to individual dyes. Electrochemical impedance spectroscopy (EIS) analysis has been executed to find the charge transfer resistance, total bulk resistance, recombination loss through Nyquist plots and Bode plots. These characteristics pretense as the mixed dye has an eminent rate of electron transportation and lower recombination loss with longer electron lifetime. The photon to electrical power conversion efficiencies of purple cabbage, spinach, turmeric and their mix dyes are explored as 0.1015%, 0.1312%, 0.3045%, and 0.602%, respectively under same simulated light condition. The mixed dye reveals the stable performance of the cell with the highest conversion efficiency due to the absorption of an extensive range of the solar spectrum and well-suited electrochemical responses.

Keywords. DSSC; chemical bath deposition; cyclic voltammetry; electrochemical impedance spectra (EIS); energy band position; photo sensitizing properties.

1. Introduction

The DSSC is an economical photo-electro-chemical cell. Dye-sensitization is a process which is analogous to photosynthesis. As a renewable energy source, DSSC has attracted great awareness over the past decade mainly due to their low production cost with high efficiency (>11%) [1]. Performance of the cells depends on all the essential components like transparent conductive oxide (TCO) substrate, photo-anode, cathode, dye, and electrolyte. The most important component in DSSC, photo-anode collects and transfers the excited photo-electrons from dye to the TCO via semiconductor metal oxide (SMO) layer [2]. A well-known nanostructured SMO, TiO_2 is used as a photo-anode, which is more efficient for a photon to electron conversion, but electron transfer rate of TiO_2 is low. This effects high interface recombination reactions between SMO, dye and electrolyte and that drops the efficiency of the system [3–7].

The resulting current due to the recombination is known as the dark current [7]. Another photo-anode material, nanostructured ZnO can create a direct electron flow path which leads to increase electron mobility and lifetime [8–10]. Nanostructured ZnO can be synthesized by many methods, and among them, a simple and cost-effective wet chemical bath deposition (CBD) method is followed to fabricate nanostructured ZnO as a photo-anode in DSSC [11]. The

*For correspondence
Published online: 08 July 2020

DSSC is fabricated by sandwiching the photo-anode, dye, electrolyte and counter electrode. At illuminated condition, electrons of the dye molecules are excited, and these electrons are transferred to the conduction band of SMO. For regeneration of the dye, electrons are supplied by the electrolyte in the reduction process. On the other hand, the electrolyte is renewed by receiving electrons flowing through counter electrode by accepting the electrons from the conduction band of SMO when the circuit is closed through the external wire with or without load [12]. This manuscript intends to reveal the performance of the DSSC with nano-structured ZnO as photo-anode material and mixed natural dye as a photo-sensitizer. The natural dyes are easy availability, low cost, biodegradable, non-toxic materials and they can synthesize easily in compare with other ruthenium based dye [13]. The wide bandgap semiconductors can easily be sensitized using different natural dyes and their mixture due to light absorption in visible to UV region [14]. Different parts of plants like leaf, flower, root, fruit, etc. are used to extract natural dyes which contain different pigments such as anthocyanin, betacyanin, chlorophyll, etc. [15–19]. Anthocyanin is a natural plant pigment and also known as flavonoids. The molecule of this group can absorb the yellow, green and blue portions of the visible spectrum for which dye appears purplish red. Betalains are a type of red and yellow indole-derived pigments and are of two categories [20]–(i) betacyanins which comprise the reddish to violet and (ii) betaxanthins, which appear yellow to orange pigments. Apart from different sources, betaxanthin presents in the stem of turmeric. In this paper, it is considered that anthocyanin, chlorophyll and betaxanthin are acquired from fresh purple cabbage (*Brassica oleracea var. capital f. rubra),* spinach (*Spinacia oleracea*) leaves and turmeric (*Curcumina longa*) stem respectively. The extracted dyes from purple cabbage, spinach and turmeric are mixed to improve visible light absorption capability. The sandwich type solar cell will be fabricated using nanostructured ZnO coated fluorine-doped tin oxide (FTO) glass substrate and the electrical parameters have been evaluated for the mixed dye.

2. Experiments

2.1 *Synthesis of ZnO nanostructure*

The FTO glass slides of rectangular shape with transparency 80% and sheet resistance 12 Ω/sq were immersed in a chemical bath consisting of 40 ml of aqueous 0.1 (M)$Zn(NO_3)_2{\cdot}6H_2O$ and 2 ml of 28% aqueous NH_4OH solution via CBD technique. A similar process for nanostructured ZnO fabrication on the glass substrate was explained by De and Sarkar [11]. In this process, ZnO nanoparticles were deposited on the conducting surface of FTO substrate at the hot plate maintaining a constant temperature of 80°C for 12 h. The coated FTOs were taken out from the solution and cleaned with deionized water until its pH becomes neutral. The ZnO coated FTOs were then placed in an oven operating at a constant temperature of 70°C for drying of the substrates. Finally, dried ZnO coated FTO substrates were annealed at 450°C for 2 h. Figure 1 shows the flowchart for the synthesis process of nanostructured ZnO photo-anode through CBD technique. The morphology of the ZnO depends on the concentration of NH_4OH, the volume of the solution, reaction time and temperature and the substrate effect. The X-ray diffraction (XRD) of the synthesized ZnO particles were performed using Cu Kα radiation in a Bruker D8 diffractometer, and the morphological and elemental analysis were executed using field emission scanning electron microscope (FESEM, Carl Zeiss SUPRA^{TM} 40).

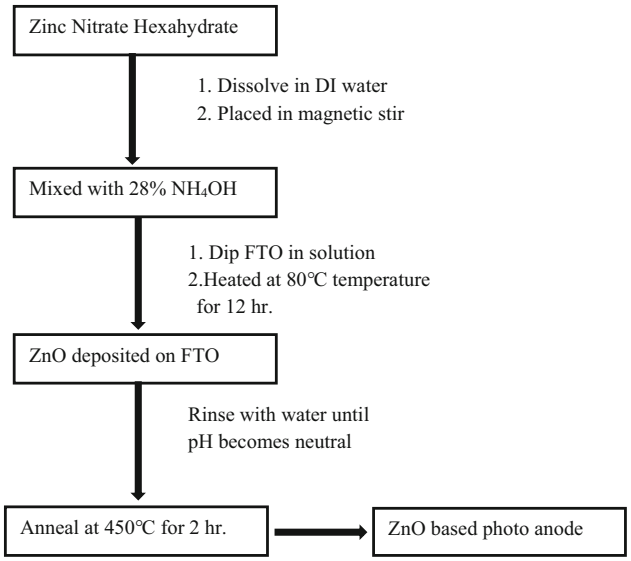

Figure 1. Flowchart for the synthesis of nanostructured ZnO photo anode.

2.2 *Extractions of natural dyes*

The extraction of natural dyes is explained in our paper Sinha *et al* [21]. The extraction of dyes from fresh purple cabbage, spinach leaves and turmeric stem are extracted individually, and in ethanolic solution, their pH comes as 7.03, 7.2 and 8.5, respectively. The mixture of the extracted individual dyes in a crude form at the ratio of 1:1:1 proportion and the whole mixture is added to ethanol in the same proportion. It is then stirred for 10 minutes and filtered. The pH of the mixed dye comes as 7.1. The light absorption characteristics of individual dyes and their mixed counterpart are observed using UV-vis (UV-3600, Shimadju, Japan) spectroscopy at room temperature. The nanostructured ZnO coated FTO substrates are dipped into the dyes separately for 24 h, and after removal from the dyes, the dye-loaded ZnO photo anodes are rinsed thoroughly with DI water and dried at room temperature. The chemical structures of the dyes are shown in figure 2.

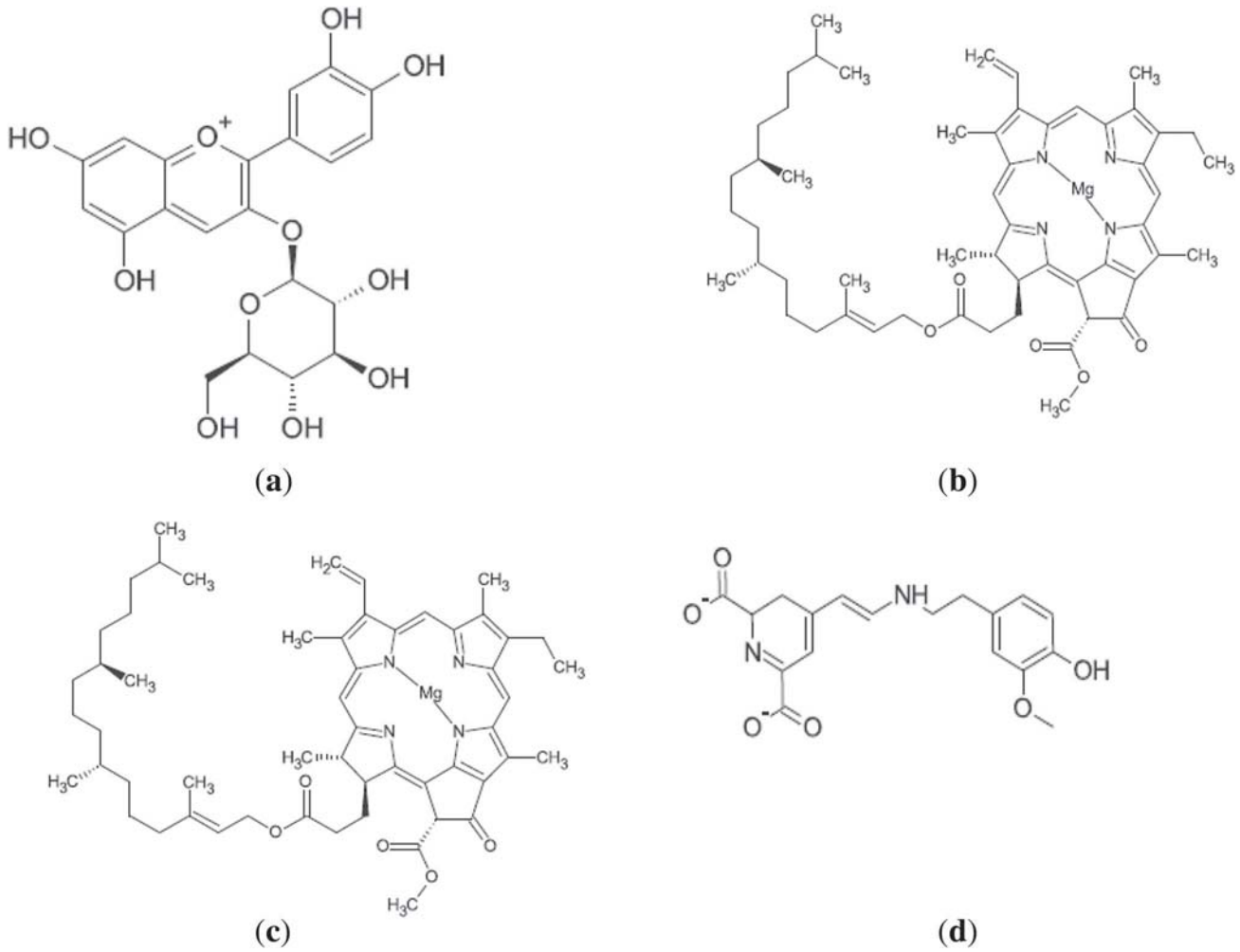

Figure 2. Chemical structure of (**A**) Anthocyanin [22], (**B**) Chlorophyll a, [22], (**C**) Chlorophyll b [23] and (**D**) Betaxanthin dye [21].

2.3 *Fabrication of DSSC*

The DSSCs (operative cell area 1 cm^2) are fabricated by unifying synthesized ZnO based photo anode dipped with natural dye sensitizer, and a few drops of Iodine based redox couple (I^-/I_3^-) is added as an electrolyte. Another FTO of the same size and same specification is considered for the counter electrode for these cells. The counter electrode or cathode of the cell is coated with carbon. Carbon acts as a catalyst for enhancement of electron flow from the counter electrode to the electrolyte. The generated current and voltage (I-V) characteristics of the DSSCs are measured through a source meter (2400, Keithley, USA) and a solar simulator of light energy 100 mW/cm^2.

3. Results and discussion

3.1 *Microstructure of ZnO*

The FESEM image of ZnO surface layer synthesized on FTO (refer to figure 3a), shows that two types of nanostructures—nano-wire and nano-plate are present. The average height of ZnO nano-wire is 5 μm and width is 200 nm, and they are slanted towards different directions. The average length of nano-plate is ∼5 μm and thickness is ∼50 nm. The crystalline structure of the ZnO particles have been evaluated by XRD, and the pattern has been shown in figure 3b. It shows a standard hexagonal wurtzite ZnO structure (JCPDS card no. 75-1526). The crystallite size (D) and lattice strain (ε) are calculated from the Scherrer and tangent formula respectively and shown in eq. (2) and eq. (3) [24, 25].

$$D = \frac{0.9\lambda}{\beta Cos\theta} \tag{2}$$

$$\varepsilon = \frac{\beta}{4tan\theta} \tag{3}$$

Lattice parameters for the wurtzite structure (a and c) are calculated from the eq. (4) and eq. (5) [26, 27]

$$a = \frac{\lambda}{\sqrt[3]{3}Sin\theta} \tag{4}$$

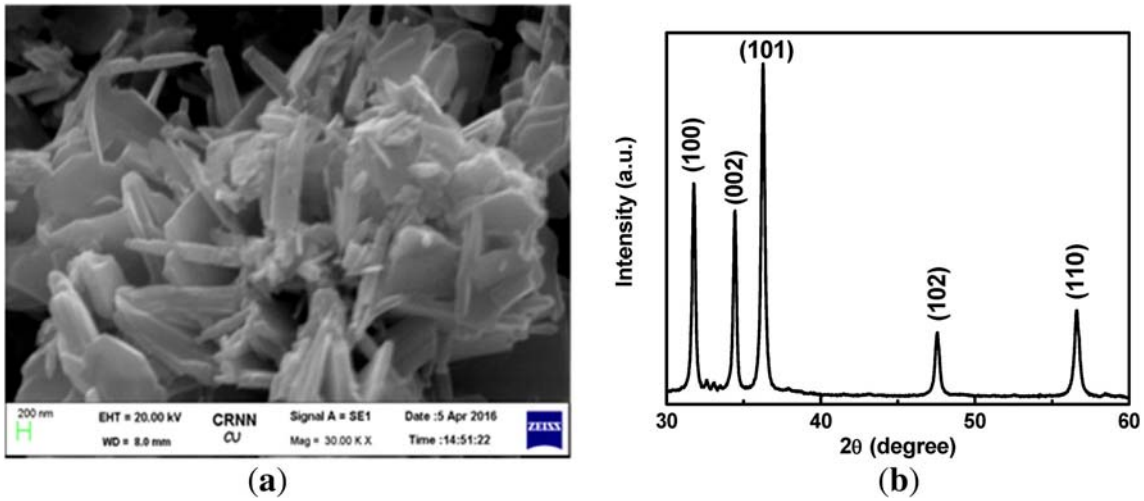

Figure 3. (**a**) FESEM image of the nanostructured ZnO coated on FTO glass; (**b**) XRD pattern of synthesized ZnO.

$$c = \frac{\lambda}{Sin\theta} \tag{5}$$

Considering the three main peaks at (101), (002) and (100), the average crystallite size (D) is ∼45 nm, average lattice strain (ε) 0.1829, and the calculated lattice constants are a = 0.3667 nm and c = 0.5288 nm. The D-value of the sample is comparing well with the average thickness of the nano-plates.

3.2 *Photo sensitizing properties of natural dyes*

Photo sensitizing properties of purple cabbage (anthocyanin), spinach (chlorophyll), turmeric (betaxanthin) and their mixed combination are apprehended through FTIR and UV-vis spectroscopy. The FTIR spectra of mixed natural dye loaded ZnO substrate accounted at the band of 4000 to 400 cm^{-1} and shown in figure 4. The spectra represent a wide spread absorption in the range of 3369-3416 cm^{-1} with a peak at 3407 cm^{-1} that is ascribed to the stretching vibration of –OH [28] and –NH bonds. A slight absorption of 2922 cm^{-1} is credited to –CH stretching vibration. A wide absorption band at 1617-1667 cm^{-1} with, a peak of 1645 cm^{-1}, is owed to C=O conjugated vibration bond. The absorption bands at 1025-1082 cm^{-1} and 1376-1419 cm^{-1} with peaks at 1053 cm^{-1} and 1378 cm^{-1} are attributed to C-C and C-N bonding respectively. A peak at 486 cm^{-1} attributes Zn-O bonding. From the literature, spinach [23] consists chlorophyll a and chlorophyll b, and has the peaks of O-H stretching vibration, C-H stretching and bending vibration of chlorophyll, C=O bonding, C-C and C-N vibration of tetra pyrrole ring of chlorophyll. Purple cabbage consisting anthocyanin [29] shows stretching vibration of C-H bond, C=O bonding and phenolic O-H stretching vibration of anthocyanin. Turmeric consists betaxanthin [21] shows the O-H, N-H and C-H

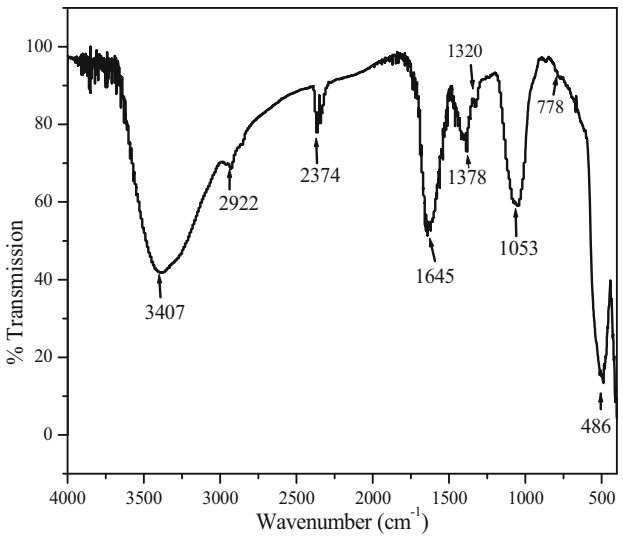

Figure 4. FTIR spectra of Mixed dye containing anchoring groups on ZnO substrate.

stretching vibration, C=O and C=C bonding and bending vibration of enol and keto part of C-OH and C≡CH. Enol and keto tautomerism have been observed in betaxanthin dye. From the FTIR spectra, it can be summarized that the mixed dye contains all the anchoring groups of the individual dyes, i.e., hydroxyl, carbonyl, methyl, and amine groups, which can anchor firmly with ZnO and increase electron mobility.

It is exposed from the UV-vis spectrum analysis (figure 5a) that purple cabbage (PC) possesses a wide spread absorption band at 450-690 nm with peaks at 512 nm and 650 nm. Comparable spectrum was demonstrated by Chang *et al* and Syafinara *et al* [22, 30]. The spinach (SP) exhibits absorption bands at lower (λ = 410–445 nm and 450-500 nm) as well as the higher wavelength (λ = 580-700 nm).

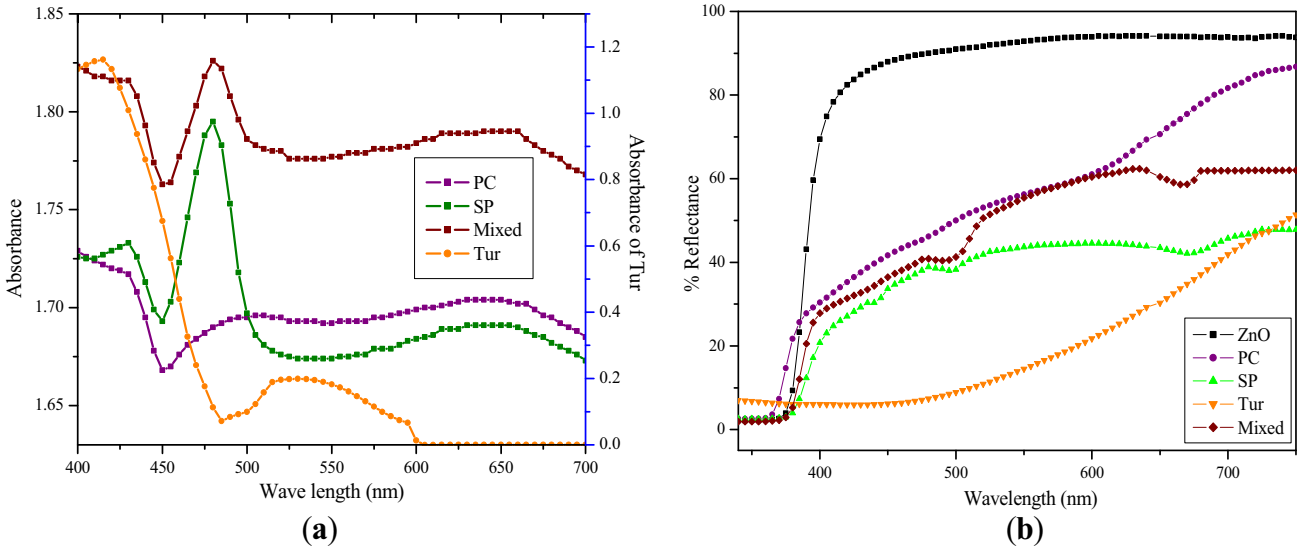

Figure 5. (**a**) UV-Vis absorption spectra of purple cabbage, spinach, turmeric and their mixed one with different peak positions; (**b**) DRS of Zinc oxide film with and without loading of different natural dyes show peak shifting.

It shows three peaks at 430 nm, 485 nm and 655 nm. A similar spectrum of spinach was exposed by Sengupta *et al* [23]. Turmeric (Tur) absorbs light at lower (λ = 350-450 nm) to medium regions (λ = 500-600 nm) with the peak absorbance at λ = 415 nm and 515 nm [21]. Similar spectrum was also shown by Kim *et al* [31]. The mixed dye of these three (Mixed) can absorb a band of λ = 380-445 nm, λ = 450-510 nm and also at λ = 575-700 nm. These spectra have shown three peaks at 433 nm, 484 nm and 652 nm with different absorbance. It is well known that ZnO has photon absorption quality in UV region, i.e., below 400 nm wavelength. At visible region it can adequately reflect the light, i.e., diffused reflectance spectra (DRS) is almost 95%. The natural dyes loaded with ZnO yield lower DRS due to light harvested by the dyes. Figure 5b proclaims the DRS of equal thickened ZnO films with and without dye loading. The UV-vis absorption spectra of individual dyes are compared with their DRS in figure 6. It is observed from the figure 6a that the absorbance peak of purple cabbage shifts from 512 nm to 485 nm and 650 nm to 626 nm in its DRS after dye loading in zinc oxide film. The absorption peak of spinach has shifted from 430 nm to 445 nm, 485 nm to 500 nm and 655 nm to 670 nm in their DRS after dye loading in zinc oxide film (refers to figure 6b). Similarly, 415 nm and 515 nm of absorption peaks of turmeric are shifted to 425 nm and 526 nm in DRS. The absorption peaks (433 nm 484 nm and 652 nm) of mixed dye are shifted to 441 nm, 493 nm and 660 nm, respectively, in DRS. The shifting of the absorption peak occurs due to different chemical groups presents in the dyes and the bonding of dyes with ZnO surface. Similar work has reported by Sengupta *et al* [23].

The realization of the band-gap energies of the natural dyes can be possible from Tauc's relation [32] shown in eq. (6). The Tauc's plot is related with the photon energy (hν) on the x-axis, and the quantity $(\alpha h\nu)^{1/n}$ on the y-axis and bandgap energies can be calculated by extrapolation of the linear region to zero absorbance (shown in figure 7).

$$(\alpha h\nu)^{1/n} = (h\nu - E_g) \tag{6}$$

Here α is the absorbance coefficient, obtained by the UV-vis spectroscopy and n is considered as 0.5.

The optical bandgap energy E_{gopt} can be calculated from the Plank's constant (h), velocity of the light (c) and wavelength of maximum absorbance ($\lambda_{onstate}$) and expressed is the equation (7).

$$E_{gopt} = \left(\frac{h \times c}{\lambda_{onstate}}\right) \tag{7}$$

3.3 *Cyclic voltammetry*

The successful electron transport from dye to SMO determines the generation of photo current from the cell. For the electron transport, lowest unoccupied molecular orbital (LUMO) position of the dye should be above the conduction band of SMO, and for hole transport, the highest occupied molecular orbital (HOMO) position of dye should be above the valence band of SMO. This arrangement can enhance the electron flow from dye to SMO and reduce the recombination loss of SMO and improve the stability of the cell [33]. Cyclic voltammeter can measure the redox characteristics of the dye. HOMO is considered as an oxidation process and the energy required to drag out an electron from a molecule of dye whereas LUMO is a reduction process and the energy necessitates to insert an

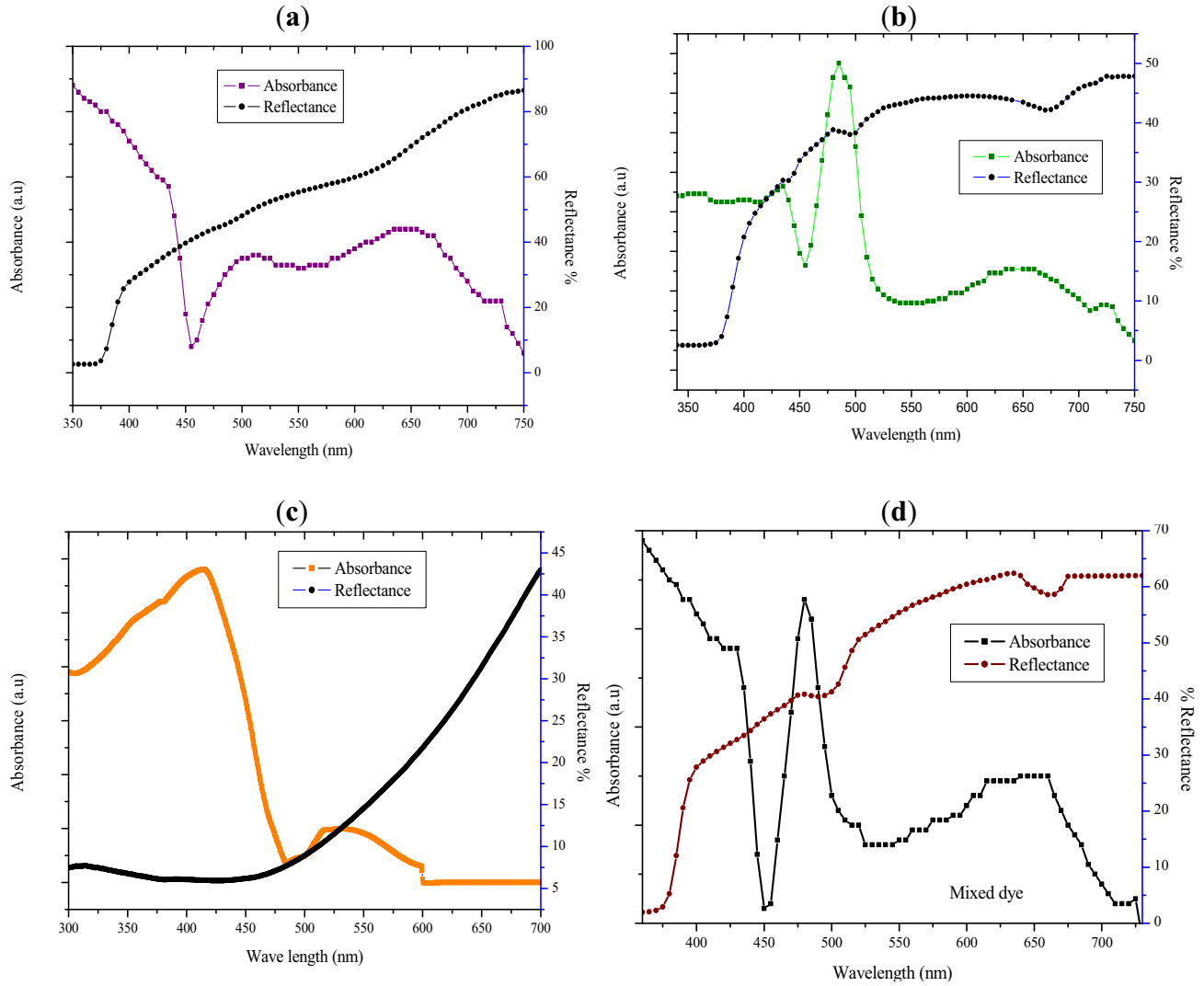

Figure 6. Comparison of UV-vis absorbance spectra of different dyes with their DRS, loaded with zinc oxide films. (**a**) Purple Cabbage (PC), (**b**) Spinach (SP), (**c**) Turmeric (Tur) and (**d**) Mixed of three dyes.

electron to a dye molecule. The difference between HOMO and LUMO level in the energy band describes the band gap energy of the dye. The measurements of cyclic voltammetry have been done using three electrodes method [CH Instrument 1120A]. As a working electrode platinum is used and platinum wire of 3 mm diameter is considered for the counter electrode. $Ag/AgCl_2$ has been taken as a reference electrode with 0.1M Tetra butyl ammonium perchlorate as supporting electrolyte under nitrogen environment. For the extraction of the dyes, Acetonitrile (SP and Tur) and Millipore water (PC and Mixed) are used as a solvent. The experiment is carried out at room temperature (25°C) and at a scan rate of 100 mV/Sec. The redox reaction for the dyes are shown in figure 8a and b. It shows that the reaction of the dyes are entirely irreversible (i.e., $i_a >> i_c$). The oxidation process of the dye molecules takes place at their anodic potential, and after reduction process, they return to their original form. The molecule attached to the surface of the working electrode is entirely changed after oxidation as the response is irreversible. As a known reference, Ferrocene is considered, and at absolute vacuum, its value is taken as −4.4 eV, HOMO and LUMO energy levels of the dyes are derived [29] in eqs. (8) and (9) and shown in table 1.

$$E_{(HOMO)} = -[E_{ox} + 4.4] \text{ eV} \tag{8}$$

$$E_{(LUMO)} = -[E_{red} + 4.4] \text{ eV} \tag{9}$$

The photo induced electron transfer process was introduced by Rehm-Weller [34] which can determine the driving force (ΔG°) of the energy transfer between a donor and an acceptor and it is shown in eq. (10).

$$\Delta G^0 = e[E_{ox}(dye) - E_{red}(SMO)] - \Delta E \tag{10}$$

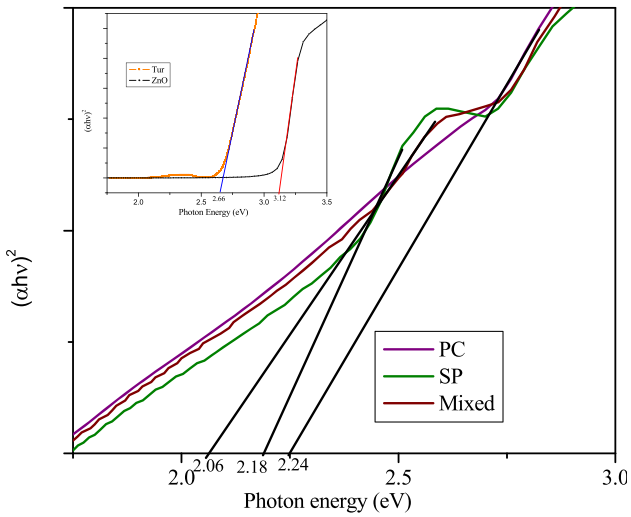

Figure 7. Tauc's plot for the purple cabbage, spinach and mixed dye and inset turmeric and ZnO.

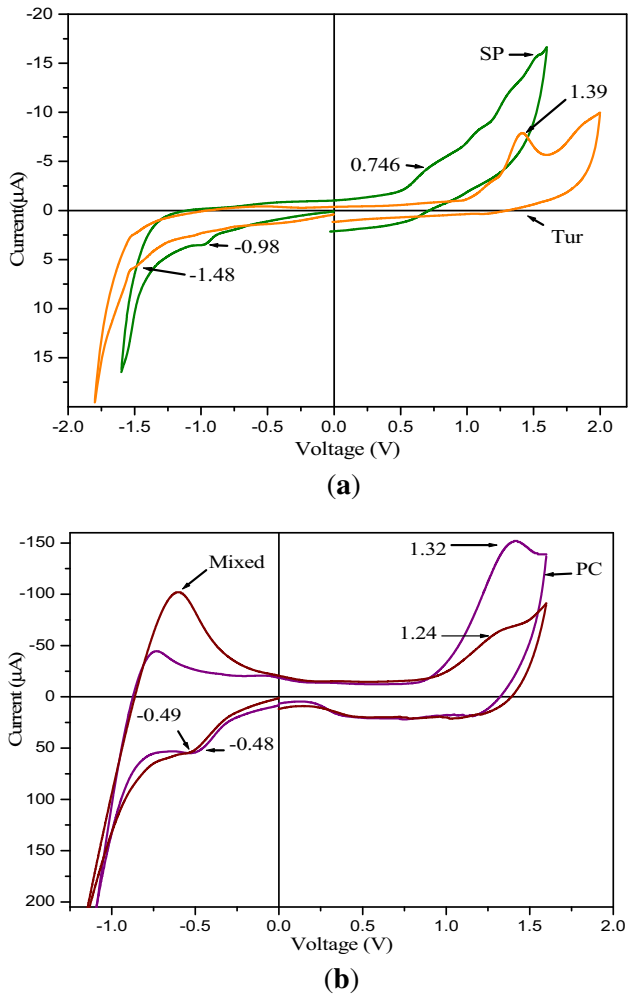

Figure 8. Cyclic voltammetry diagram of (**a**) spinach (SP) and turmeric (Tur) dye and (**b**) purple cabbage (PC) and mixed dye with their oxidation and reduction peaks.

The energy requirement for the shifting of an electron from dye to ZnO surface is evaluated and shown in table 1.

The bandgap energies of the mixed dye achieved from Tauc's plot, and CV indicates relatively lower values (2.06 eV and 1.73 eV) in comparison with other dyes. It also possesses high electron affinity (3.91 eV) with moderately high oxidation peak (1.24 eV), and prerequisite of driving force energy is low (0.34 eV) for spontaneous transmission of an electron from dye to SMO. Though the oxidation peak of purple cabbage (1.32) is higher than the mixed dye and the driving force energy is also required less (0.34 eV), the other parameters, i.e., required bandgap energy is more. On the other hand, turmeric possesses high electron affinity (2.92) with a comprehensive band gap energy, and it needed a high driving force energy (1.34 eV) to transfer an electron from dye to SMO. Spinach also has a low bandgap energy (1.73 eV) and quietly adequate driving force energy (0.84 eV). The mixed dye has the better shares of all the individual dyes, and it has high stability, and it is more applicable for fabrication of DSSC. Table 1 is associated with the bandgap energies from different methods with energy band positions and driving force energies of the extracted natural dyes. Figure 9 shows the energy band diagram of all the components associated with dye-sensitized solar cell with different natural dyes and their mixture. From literature [4], the conduction band position of ZnO is considered as -4.26 eV and the Tauc's plot and E_{gopt}, provide bandgap energy of 3.12 eV for the synthesized ZnO. Now the valence band position is calculated as $\sim(-7.38$ eV).

3.4 *Photo conversion efficiencies of fabricated cells*

The performances of the fabricated cells are evaluated in terms of photo conversion efficiency (η) and fill factor calculated from their I-V and P-V characteristics. Efficiency is achieved from maximum power generated from the cell concerning light energy provided by the solar simulator (100 mW/cm^2). Fill factor is the ratio of maximum effective power to the multiplication of generated short circuit current and open circuit voltage. The dyes are playing a significant role to decide the efficiency of the cell with their photo absorbance criteria and presence of different anchoring groups. The I-V and P-V characteristics of the fabricated DSSCs with different dyes are shown in figure 10a and b, respectively and the outcomes are placed in table 2. Purple cabbage has significantly low short circuit current but moderately high open circuit voltage, whereas, spinach has a better short circuit current, but a more moderate open circuit voltage and turmeric show better performance over purple cabbage and spinach. As the dyes are not over sensitive to each other, the mixed dye cell provides the best performance ($\eta = 0.602\%$ and the fill

Table 1. Bandgap energies, energy band positions and driving force energies of different extracted dyes.

Dye	E_g from Tauc's plot) eV	E_{gopt} (eV)	E_g from CV (eV)	HOMO position	LUMO position	Driving force energy (eV)
Purple cabbage	2.24	2	1.8	−5.72	−3.92	0.34
Spinach	2.18	2.59	1.73	−5.15	−3.42	0.84
Turmeric	2.66	3.01	2.87	−5.79	−2.92	1.34
Mixed dye	2.06	2.58	1.73	−5.64	−3.91	0.34

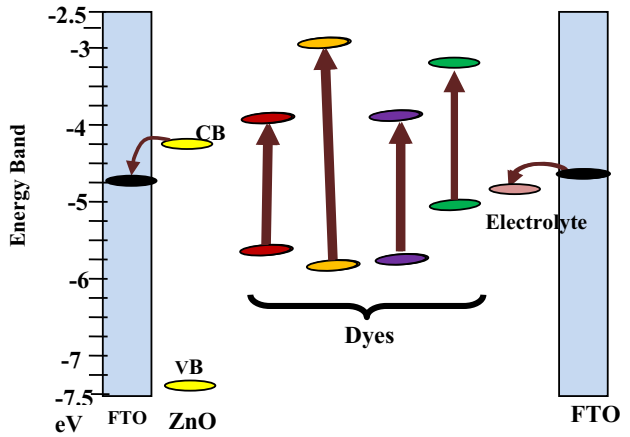

Figure 9. Energy band diagram of dye-sensitized solar cell with natural dyes and their mixture.

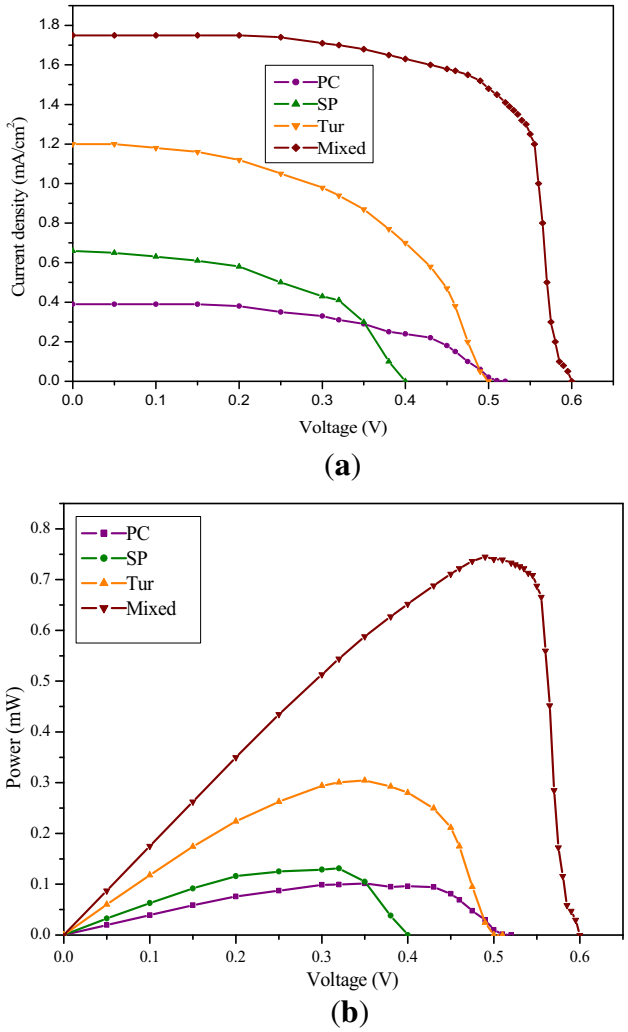

Figure 10. (**a**) I-V and (**b**) P-V characteristics of DSSC with purple cabbage, spinach, turmeric and their mixture.

factor of 0.68) over these individual dyes due to the absorbance of a broad band of light energy and presence of all the anchoring groups of individual.

3.5 *Electrochemical impedance spectroscopy (EIS)*

It is a method of characterizing electrochemical properties of materials and their interfaces. It is used for characteristics of electrode processes and complex interfaces in which physical and chemical behaviour is dependent. Faradaic impedance spectra presented as Nyquist plot (Zreal vs Zimg) which can indicate the electron transfer resistive behaviour of the dye. EIS analysis is carried out for the developed cells to realize this behaviour. Figure 11a shows the Nyquist plots of the cells and figure 11b is the best fitted equivalent circuit of the EIS spectra. The Nyquist plots of the cells are associated with two semicircles (due to RC parallel circuit) and a straight line with a slope. These semicircles and the straight line are initiated at high, medium and low frequencies according to redox reactions at counter electrode-electrolyte interface (R2 and C2 parallel circuit), ZnO-dye-electrolyte interface (R3 and C3 parallel circuit) and Warburg dispersion method (R4) of I^-/I_3^-, respectively. The sheet resistance (R1) of the FTO substrate is signified by the first shifting of the spectra from the origin. Consider FTOs with the same thickness of ZnO and other properties, R1 values are almost same for all the cells. R2 and R3 are called the charge transfer resistance, and C2 and C3 are the chemical capacitance for redox reaction for the said interfaces. The parameter values of the different cells are shown in table 3.

Table 2. Performance analysis of DSSC with different natural dyes.

Dyes	V_{mp} (V)	I_{mp} (mA/cm^2)	V_{oc} (V)	I_{sc} (mA/cm^2)	FF	% η
Purple cabbage	0.35	0.29	0.521	0.39	0.5	0.1015
Spinach	0.32	0.41	0.4	0.66	0.5	0.1312
Turmeric	0.35	0.87	0.5	1.2	0.51	0.3045
Mixed	0.43	1.4	0.53	1.65	0.68	0.602

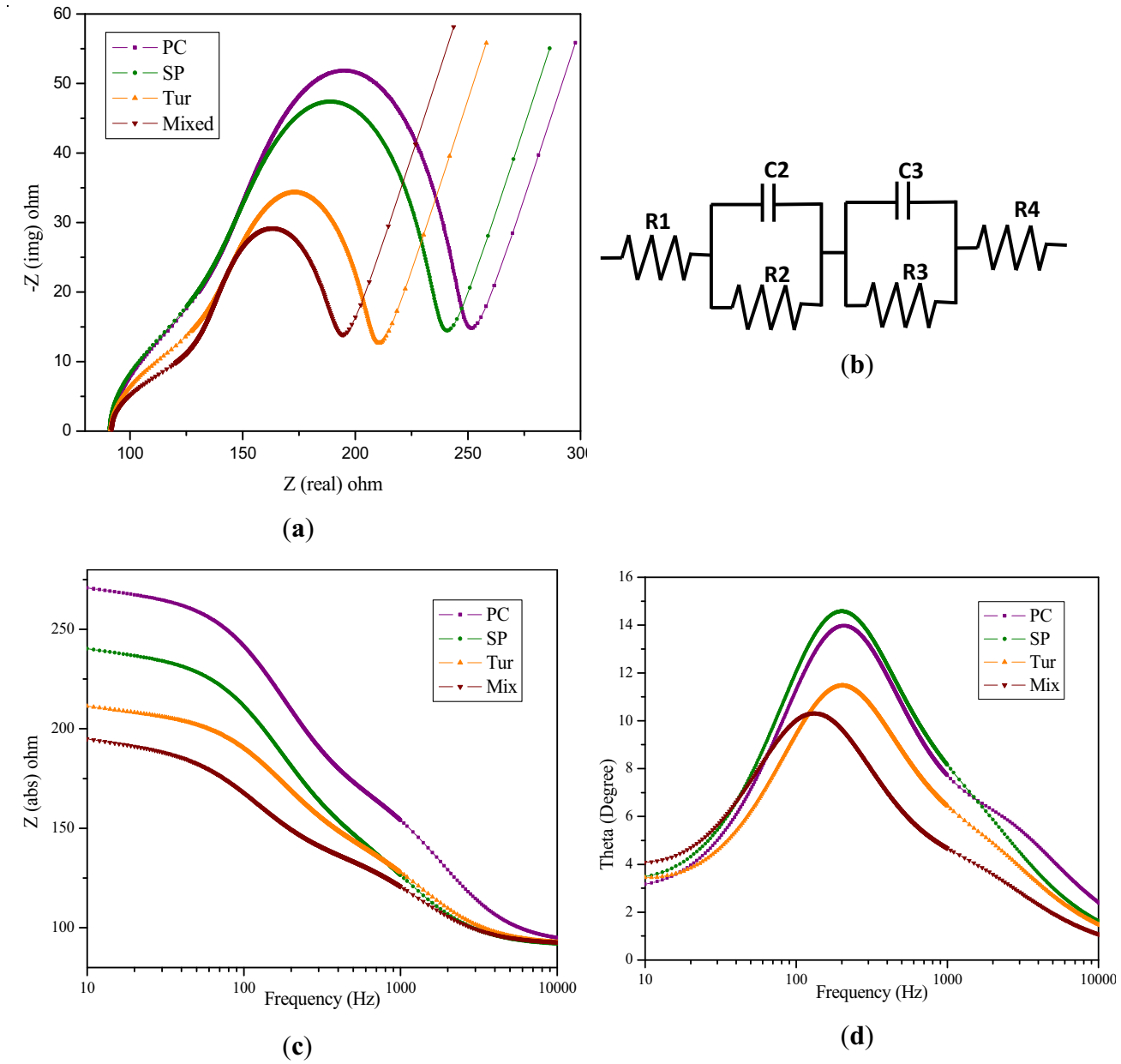

Figure 11. (**a**) Nyquist plots for fabricated cells; (**b**) Equivalent circuit of the Nyquist plots with best fitted; (**c**) Magnitude plot of Bode; (**d**) Phase plot of Bode.

It is exposed from the figure 11a and table 3 that the charge transfer resistance (R2) in carbon coated counter electrode-electrolyte interfaces is almost comparable in all cells but the charge transfer resistance (R3) is much lower in a mixed cell with respect of other cells, which implies faster electron transportation in the ZnO-dye-electrolyte

Table 3. Parameters of the equivalent circuit for Nyquist plot.

Dye	R1 (Ω)	R2 (Ω)	R3 (Ω)	C2 (F)	C3 (F)	R4 (Ω)	Electron lifetime (ms)
PC	91.94	52.7	97.4	2.135E−6	10.77E−6	120.9	1.048
SP	90.9	52.3	88.28	2.48E−6	11.993E−6	97.3	1.058
Tur	91.4	48.5	62.6	2.234E−6	15.7E−6	98.7	0.982
Mixed	91.76	42.2	51.7	2.84E−6	36.73E−6	102.8	1.432

Table 4. Comparison of the performance of DSSC with different dyes and different photo anodes.

Dye	I_{sc} (mA/cm^2)	V_{oc} (V)	FF	% η	Photo anode	Ref
Begonia	0.63	0.537	0.72	0.24	TiO_2	[41]
Mangosteen pericarp	2.69	0.686	0.633	1.17	TiO_2	[42]
Pink Rhododendron flowers	0.85	0.544	0.72	0.33	TiO_2	[43]
Hibiscus	1.63	0.404	0.57	0.37	TiO_2	[44]
Shisonin	4.8	0.53	0.51	1.31	TiO_2	[45]
Red turnip	9.5	0.43	0.37	1.7	TiO_2	[14]
Wild sicilian	8.2	0.38	0.38	1.19	TiO_2	[14]
RhoeoSpathacea	10.9	0.5	0.27	1.49	TiO_2	[46]
Wormwood	0.196	0.585	0.47	0.538	TiO_2	[22]
Purple cabbage	0.208	0.66	0.53	0.75	TiO_2	[22]
Turmeric	1.005	0.56	0.64	0.36	TiO_2	[20]
Beet	0.75	0.453	0.58	0.197	ZnO	[23]
Citrus leaf dye extract	0.011	0.211	0.71	0.16	TiO_2	[41]
Shisonin and chlorophyll	4.80	0.534	0.51	1.31	TiO_2	[45]
Wormwood and purple cabbage	3.16	0.66	0.62	1.29	TiO_2	[22]
Red-cabbage and curcumin	0.81	0.53	0.69	0.60	TiO_2	[18]
Spinach and Beet root	1.244	0.412	0.575	0.294	ZnO	[22]
Purple cabbage and beet root	0.89	0.43	0.6	0.3824	ZnO	[47]
Purple cabbage and spinach	1.45	0.532	0.67	0.517	ZnO	[48]
Purple cabbage, Spinach and Turmeric	1.65	0.53	0.68	0.602	ZnO	Present work

interfaces. The electron lifetime (τ) is calculated from charge transfer resistance (R3) and chemical capacitance (C3) shown in eq. (11) [35, 36].

$$\tau = R3 \times C3 \tag{11}$$

From the table 3, it is revealed that the electron lifetime is more in the cell prepared by the mixed dye. The bulk resistance of the cell can be derived by the diameter of the semicircle of the Nyquist plot. The Nyquist plot for DSSC reported elsewhere [37, 38]. The Bode plot consists magnitude plot [figure 11c] and phase plot [figure 11d]. The variation of the bulk resistance with frequency can also be obtained from Zabs and frequency plot shown in figure 11c.

At 10 Hz frequency the bulk resistance of purple cabbage, spinach, turmeric and mixed dye made cells have 270 Ω, 240 Ω, 211 Ω and 195 Ω, respectively. From the phase-frequency plot (figure 11d) the characteristics frequency peak for the electron transportation at ZnO-dye-electrolyte interface is shifted to lower frequency for mixed dye cell, which implies that the charge recombination rate is lower [39, 40], and this cell leads to its higher photo conversion efficiency with higher electron lifetime.

Table 4 shows the comparison study of the performance of DSSCs based on different natural dyes containing anthocyanin, betanin and chlorophyll pigments using different photo anode.

The main intent of this paper is to establish mixed natural dyes in a specific ratio (1:1:1) which are stable and can enhance the efficiency of DSSC. A simple natural dye fails to absorb the light in a broader wavelength of UV-visible region; hence-forth the mixed dye is established in different absorbance region or compatible to each other to show better performance rather than the individual ones. We have analyzed several dyes and their mixed ones. Some dyes are not compatible to other and provide worst response (i.e., *Butea monosperma*). Some dyes are congruent but fail to give a better response. The mixture of Purple Cabbage, Spinach and Turmeric equip the broad light absorbance within the UV-visible range. However, the cyclic voltammetry is done to enquire out the stability of the mixed ones. The mixed dye reveals lower impedance spectra and the

gain accompanied by the individual dyes which boost up the enactment of simple ones with the mixed ones.

4. Conclusions

In this paper, DSSC is prepared from cost-effective natural dyes and effortlessly synthesized ZnO nano-particle through CBD technique. The naturals dyes (purple cabbage, spinach and turmeric) are used here can absorb light in three different regions and are non-reactive to each other. Hence the mixed one has an extensive range of light absorbance and exhibits comparatively low DRS after anchored with ZnO. Cyclic voltammetry measurement supports the favorable HOMO and LUMO positions and confirms the stability of the mixed dye. The driving force energy requirement is explored less (0.34 eV) for easy transportation of electron from dye to SMO. Substantially encouraging band gap energies of the dyes are calculated from different methods. EIS analysis has supported low charge transfer resistance, lower total bulk resistance, lesser recombination loss and longer electron lifetime of the mixed dye in comparison with other individual dyes through Nyquist plots and Bode plots. These fabricated DSSC cells are characterized by I-V and P-V curves at an irradiance of 100 mW/cm^2. The mixed dye cell provides the highest cell efficiency of 0.602% with FF of 0.68.

References

[1] Sima C, Grigoriu C and Antohe S 2010 Comparison of the dye-sensitized solar cells performances based on transparent conductive ITO and FTO. *Thin Solid Films* 519: 595–597, https://doi.org/10.1016/j.tsf.2010.07.002

[2] Hoffmann M R, Martin S T, Choi W and Bahnemann D W 1995 Environmental applications of semiconductor photocatalysis. *Chem. Rev.* 95: 69–96, https://doi.org/10.1021/cr00033a004

[3] Jiang C Y, Sun X W, Lo G Q and Kwong D L 2007 Improved dye-sensitized solar cells with a ZnO-nano flower photo anode. *Appl. Phys. Lett.* 90: 263501, https://doi.org/10.1063/1.2751588

[4] Ganesh T, Nguyen H M, Mane R S, Kim N, Shinde D V, Bhande S S, Naushad M, Hui K N and Han SH 2014 Promising ZnO based DSSC performance using HMP molecular dyes of high extinction coefficient. *Dalton Trans.* 43: 11305–11308, https://doi.org/10.1039/C4DT01179A

[5] Lai M H, Lee M W, Wang G J and Tai M F 2011 Photovoltaic performance of new-structure ZnO-nano rod dye sensitized solar cells. *Int. J. Electrochem. Sci.* 6: 2122–2130, http://www.electrochemsci.org/papers/vol6/6062122

[6] Longo C and Paoli M A 2003 Dye-sensitized solar cells: a successful combination of materials. *J. Braz. Chem. Soc.* 14: 889–901, https://doi.org/10.1590/S0103-50532003000600005.

[7] Taft M H K and Sadeghzadeh S M 2018 Dye sensitized solar cell efficiency improvement using TiO_2/nano-diamond nano composite. *Sādhanā* 43: 113, https://doi.org/10.1007/s12046-018-0914-y

[8] Afifiand A and Tabatabaei M K 2014 Efficiency investigation of dye-sensitized solar cells based on the zinc oxide nanowires. *Orient J. Chem.* 30: 155–160, https://doi.org/10.13005/ojc/300118

[9] Phuoc L H, Phuoc L H, Tho D D, Dung N T, Hien V X, Vuong D D and Chien N D 2019 Enhancement of ethanol-sensing properties of ZnO nanoplates by UV illumination. *Bull. Mater. Sci.* 42: 72, https://doi.org/10.1007/s12034-019-1756-x

[10] Balaprakash V, Gowrisankar P, Rajkumar R and Sudha S 2018 Preparation and characterization of aluminum doped zinc oxide (AZO) nano-rods. *Sādhanā* 43: 86, https://doi.org/10.1007/s12046-018-0821-2

[11] De D and Sarkar D K 2017 Superhydrophobic ZnAl double hydroxide nanostructures and ZnO films on Al and glass substrates. *Mater. Chem. Phys.* 185: 195–201, https://doi.org/10.1016/j.matchemphys.2016.10.022

[12] Gong J, Liang J and Sumathy K 2012 Review on dye sensitized solar cells (DSSCs): fundamental concepts and novel materials. *Renew. Sustain. Energy Rev.* 16: 5848–5860, http://www.sciencedirect.com/science/article/pii/S136403211200319X

[13] Chandrasekharam M, Rao S, Suresh T A M, Raghavender M, Rajkumar G, Srinivasu M and Reddy P Y 2011 High spectral response heteroleptic ruthenium (II) complexes as sensitizers for dye sensitized solar cells. *J. Chem. Sci.* 123(1): 37–46

[14] Calogero G, Marco G and Cazzanti S 2010 Efficient dyesensitized solar cells using red turnip and purple wild Sicilian prickly pear fruits. *Int. J. Mol. Sci.* 11: 254–267, https://doi.org/10.3390/ijms11010254

[15] Gomez-Ortiz N M, Vazquez-Maldonado I A, Perez-Espadas A R, Mena Rejon G J, Azamar-Barrios J A and Oskam G 2010 Dye-sensitized solar cells with natural dyes extracted from achiote seeds. *Sol. Energy Mater. Sol. Cells* 94: 40–44, https://doi.org/10.1016/j.solmat.2009.05.013

[16] Hao S, Wu J, Huang Y and Lin J 2006 Natural dyes as photosensitizers for dye-sensitized solar cell. *Sol. Energy* 80: 209–214, https://doi.org/10.1016/j.solener.2005.05.009

[17] Hug H, Bader Mair M P and Glatzel T 2014 Biophotovoltaics: natural pigments in dye-sensitized solar cells. *Appl. Energy* 115: 216–225, https://doi.org/10.1016/j.apenergy.2013.10.055

[18] Furukawa S, Iino H, Iwamoto T, Kukita K and Yamauchi S 2009 Characteristics of dye-sensitized solar cells using natural dye. *Thin Solid Films* 518: 526–529, https://doi.org/10.1016/j.tsf.2009.07.045

[19] Nwanya A C, Ugwuoke P E, Ejikeme P M, Oparaku O U and Ezema F I 2012 *Jathropha curcas* and *Citrus aurantium* leaves dye extract for use in dye sensitized solar cell with TiO_2 films. *Int. J. Electrochem. Sci.* 7: 11219–11235, http://www.electrochemsci.org/papers/vol7/71111219.pdf

[20] Salisbury Frank B and Cleon W R 1991 *Plant Physiology* (4th ed.). Wadsworth Publishing, Belmont, California, pp. 325–326, ISBN 0-534-15162-0

[21] Sinha D, De D and Ayaz A 2018 Performance and stability analysis of curcumin dye as a photo sensitizer used in

nanostructured ZnO based DSSC. *Spectrochim. Acta* 193: 467–474, https://doi.org/10.1016/j.saa.2017.12.058

[22] Chang H, Kao M J, Chen T L, Chen C H, Cho K C and Lai X R 2013 Characterization of natural dye extracted from wormwood and purple cabbage for dye-sensitized solar cells. *Int. J. Photo-Energy* 159502, https://doi.org/10.1155/2013/159502

[23] Sengupta D, Mondal B and Mukherjee K 2015 Visible light absorption and photo-sensitizing properties of spinach leaves and beetroot extracted natural dyes, *Spectrochim. Acta* 148: 85–92, https://doi.org/10.1016/j.saa.2015.03.120

[24] Chen K J, Fang T H, Hung F Y, Ji L W, Chang S J, Young S J and Hsiao Y J 2008 The crystallization and physical properties of Al doped ZnO nanoparticles. *Appl. Surf. Sci.* 254: 5791–5795, https://doi.org/10.1016/j.apsusc.2008.03.080

[25] Alexander L and Klug HP 1950 Determination of crystallite size with the X-ray spectrometer. *J. Appl. Phys*. 21: 137–142, https://doi.org/10.1063/1.1699612

[26] Suryanarayana C and Norton M G 1998 *X-ray Diffraction: A Practical Approach.* Plenum Press, New York, ISBN 978-1-4899-0148-4

[27] Sengupta D, Mondal B and Mukherjee K 2017 Genesis of flake-like morphology and dye-sensitized solar cell performance of Al-doped ZnO particles: a study. *J. Nanopart. Res.* 19: 100, https://doi.org/10.1007/s11051-017-3802-1

[28] Akın S, Açıkgöz S, Gülen M, Akyürek C and Sönmezoğlu S 2016 Investigation of the photo-induced electron injection processes for natural dye-sensitized. *Sol. Cells RSC Adv*. 685125, https://doi.org/10.1039/C6RA19653E

[29] Vernon L P and Seely G R 1966 *The Chlorophylls*. Academic Press, New York, ISBN: 9781483267722

[30] Mozaffari S A, Saeidi M and Rahmanian R 2015 Photoelectric characterization of fabricated dye-sensitized solar cell using dye extracted from red Siahkooti fruit as a natural sensitizer. *Spectrochim. Acta Part A* 142: 226–231, https://doi.org/10.1016/j.saa.2015.02.003

[31] Kim H J, Kim D J, Karthick S N, Hemalatha K V, Raj C J, Ok S and Choe Y 2013 Curcumin dye extracted from *Curcuma longa* L. used as sensitizers for efficient dye-sensitized solar cells. *Int. J. Electrochem. Sci*. 8: 8320–8328, http://www.electrochemsci.org/papers/vol8/80608320.pdf

[32] Zhao Y, Li W, Pan L, Zhai D, Wang Y, Li L, Cheng W, Yin W, Wang X, Xu J B and Shi Y 2016 ZnO-nanorods/grapheme hetero-structure: a direct electron transfer glucose biosensor. *Sci. Rep.* 6: 32327, https://doi.org/10.1038/srep32327

[33] Bredas J L, Silbey R, Boudreux D S and Chance R R 1983 Chain-length dependence of electronic and electrochemical properties of conjugated systems: polyacetylene, polyphenylene, polythiophene, and polypyrrole. *J. Am. Chem. Soc*. 105: 6555, https://doi.org/10.1021/ja00360a004

[34] Rehm D and Weller A 1970 Kinetics of fluorescence quenching by electron and H-atom transfer. *Isr. J. Chem*. 8: 259–271, https://doi.org/10.1002/ijch.197000029

[35] Wang Q, Ito S and Gratzel M 2006 Characteristics of high efficiency dye-sensitized solar cells. *J. Phys. Chem.* B 110: 25210–25221, https://doi.org/10.1021/jp064256o

[36] Das P, Sengupta D, Kasinadhuni U, Mondal B and Mukherjee K 2015 Nano-crystalline thin and nano-particulate thick TiO_2 layer: cost effective sequential deposition and study on dye sensitized solar cell characteristics. *Mater. Res. Bull.* 66: 32–38, https://doi.org/10.1016/j.materresbull.2015.02.018

[37] Hsu C P, Lee K M, Huang J T W, Lin C Y, Lee C H, Wang L P, Tsai S Y and HoK C 2008 EIS analysis on low temperature fabrication of TiO_2 porous films for dye-sensitized solar cells. *Electrochim. Acta* 53: 7514–7522 https://doi.org/10.1016/j.electacta.2008.01.104

[38] Yuan S, Li Y, Zhang Q and Wang H 2012 Anatase TiO_2 sol as a low reactive precursor to form the photoanodes with compact films of dye-sensitized solar cells. *Electrochim. Acta* 79: 182–188, https://doi.org/10.1016/j.electacta.2012.06.104

[39] Li Z, Zhou Y, Xue G, Yu T, Liu J and Zou Z 2012 Fabrication of hierarchically assembled microspheres consisting of nanoporous ZnO nanosheets for high-efficiency dye-sensitized solar cells. *J. Mater. Chem*. 22: 14341, https://doi.org/10.1039/C2JM32823B

[40] Sengupta D, Das P, Mondal B and Mukherjee K 2015 Study on the dye sensitized solar cell characteristics of zinc oxide photo-anode prepared on two different transparent conducting substrates. *Mater. Focus* 4: 379–384, https://doi.org/10.1166/mat.2015.1264

[41] Kumara N T R N, Ekanayake P, Lim A, Iskandar M and Ming L C 2013 Study of the enhancement of cell performance of dye sensitized solar cells sensitized with *Nephelium lappaceum* (F:Sapindaceae). *J. Sol. Energy Eng.* 135: 031014, https://doi.org/10.1115/1.4023877

[42] Wongcharee K, Meeyoo V and Chavadej S 2007 Dye-sensitized solar cell using natural dyes extracted from rosella and blue pea flowers. *Sol. Energy Mater. Sol. Cells* 91: 566–571, https://doi.org/10.5935/0103-5053.20140218

[43] Kim H, Bin Y, Karthick S N, Hemalatha K V C, Raj J and Venkatesan S 2013 Natural dye extracted from Rhododendron species flowers as a photosensitizer in dye sensitized solar cell. *Int. J. Electrochem. Sci*. 867: 34–43, http://www.electrochemsci.org/papers/vol8/80506734.pdf

[44] Zhou H, Wu L, Gao Y and Ma T 2011 Dye-sensitized solar cells using 20 natural dyes as sensitizers. *J. Photochem. Photobiol. A Chem.* 219: 188–194, https://doi.org/10.1016/j.jphotochem.2011.02.008

[45] Kumara G R A, Kaneko S, Okuya M, Onwona-Agyeman B, Konno A and Tennakone K 2006 Shiso leaf pigments for dye sensitized solid-state solar cell. *Sol. Energy Mater. Sol. Cells* 90: 1220–1226, https://doi.org/10.1016/j.solmat.2005.07.007

[46] Lai W H, Su Y H, Teoh L G and Hon M H 2008 Commercial and natural dyes as photosensitizers for a water-based dye sensitized solar cell loaded with gold nanoparticles. *J. Photochem. Photobiol. A Chem.* 195: 307–313, https://doi.org/10.1016/j.jphotochem.2007.10.018

[47] Sinha D, De D, Goswami D and Ayaz A 2018 Fabrication of DSSC with nanostructured ZnO photo-anode and natural dye sensitizer. *Proc. Mater. Today* 5: 2056–2063, https://doi.org/10.1016/j.matpr.2017.09.201

[48] Goswami D, Sinha D and De D 2017 Nanostructured ZnO and natural dye based DSSC for efficiency enhancement. In: *Proceeding of IEEE 3rd International Conference on Science, Technology, Engineering and Management,* pp. 556–560, https://doi.org/10.1109/ICONSTEM.2017.8261430